

Theoretical Analysis of the Mechanism and Regioselectivity of the 1,3-dipolar Cycloaddition of *E*-3-(dimethylamino)-1-(10*H*-phenothiazin-2-yl) prop-2-en-1-one with Some Nitrilimines Using DFT and the Distortion/interaction Model

Farid Moeinpour^{1,*} and Amir Khojastehnezhad²

¹ Department of Chemistry, Bandar Abbas Branch, Islamic Azad University, Bandar Abbas 7915893144, Iran

² Department of Chemistry, Islamic Azad University, Mashhad Branch, Mashhad, Iran

* Corresponding author: E-mail: f.moeinpour@gmail.com; fmoeinpour52@iauba.ac.ir

Received: 06-02-2014

Abstract

The regiochemistry of 1,3-dipolar cycloaddition reactions of *E*-3-(dimethylamino)-1-(10*H*-phenothiazin-2-yl) prop-2-en-1-one with some nitrilimines were investigated using density functional theory (DFT) -based reactivity indexes, activation energy calculations and the distortion/interaction model at B3LYP/6-311G(d,p) level of theory. Analysis of the geometries and bond orders (BOs) at the TS structures associated with the different reaction pathways shows that these 1,3-dipolar cycloaddition reactions occur via an asynchronous concerted mechanism.

Keywords: Regioselectivity; cycloaddition; DFT calculations; distortion/interaction model

1. Introduction

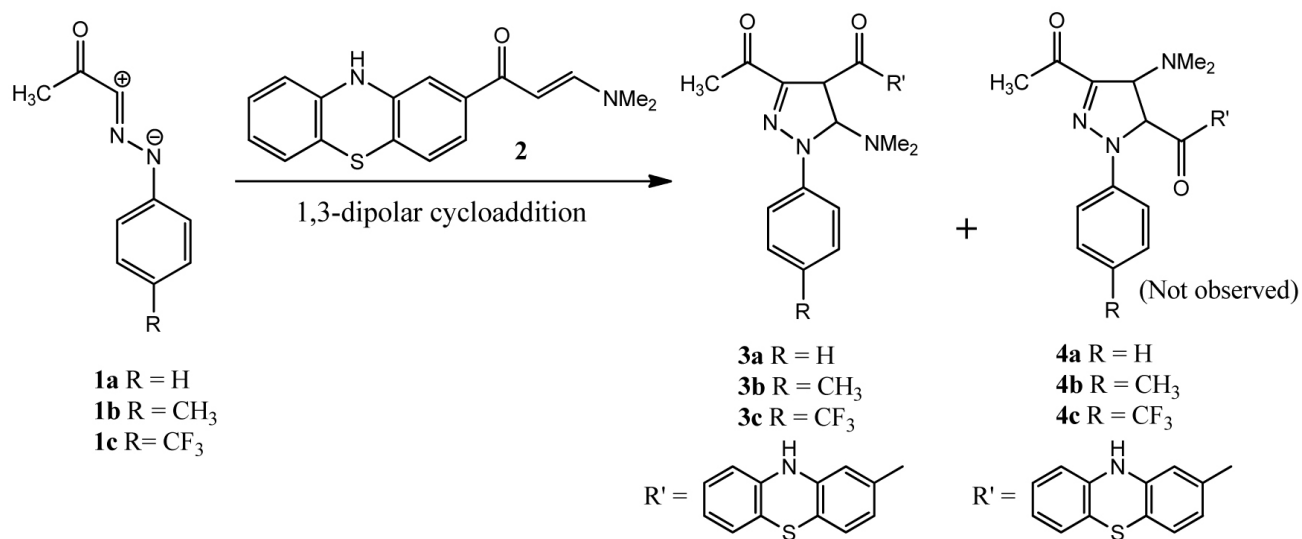
The 1,3-dipolar cycloaddition is a chemical reaction between a 1,3-dipole and a dipolarophile to form a five-membered ring.¹ These reactions are ones of the most important processes with both synthetic and mechanistic interest in organic chemistry. Current understanding of the underlying principle in the Diels–Alder reactions and the 1,3-dipolar cycloadditions (1,3-DC) has grown from valuable interaction between theory and experiment.^{2–4}

The 1,3-DC reactions possess several interesting characteristics, in particular, regioselectivity. Although transition state theory remains the most widely used and the exact approach for the study of the mechanism and the regiochemistry of these reactions, the localization of transition states is not always easy. Furthermore, transition-state calculations are often very time-consuming when bulky substituents are present in reactive systems. Reactivity descriptors based on the density functional theory (DFT), such as Fukui indexes, local softnesses and local electrophilicity, have been extensively used for the prediction of the regiochemistry. For instance, several treat-

ments of 1,3-DC reactions of nitrilimines with various dipolarophiles can be found in the literature.^{5–7} The 1,3-DC reactions of nitrilimines with alkenes is an important method for preparing pyrazoles and pyrazolidines in a regioselective and stereoselective manner.⁸ Experimentally; it has been found that the cycloaddition reactions of nitrilimines **1a–c** with *E*-3-(dimethylamino)-1-(10*H*-phenothiazin-2-yl) prop-2-en-1-one **2** give preferentially the cycloadducts **3a**, **3b** and **3c** respectively, shown in Scheme 1.⁹ In continuation of our studies on the mechanism and regioselectivity of the 1,3-DC reactions,^{10–18} we became interested in the above mentioned reactions based on activation energy calculations, the distortion/interaction model and DFT-based reactivity indexes.

2. Computational Details

All calculations were carried out with GAUSSIAN03 program suite.¹⁹ Geometry optimization of the reactants was carried out using DFT methods at the B3LYP/6-311G (d,p) level of theory.²⁰ The transition sta-



Scheme 1. The regioisomeric pathways for 1,3-dipolar cycloadditions.

tes (TSs) for the 1,3-DC reactions have been localized at the B3LYP/6-31G(d,p) level of theory. Frequency calculations characterized the stationary points to verify that the TSs had one imaginary frequency. The intrinsic reaction coordinates (IRC)²¹ calculation was performed in forward and backward path to identify that each saddle point connects to the two associated minima using the second-order González–Schlegel integration method.^{22,23} The atomic electronic populations were evaluated according to Merz–Kollman scheme (MK option).^{24,25} The electronic chemical potential μ was evaluated in terms of the one electron energies of the HOMO and LUMO, using Eq. (1):²⁶

$$\mu = \epsilon_{\text{HOMO}} + \epsilon_{\text{LUMO}}/2 \quad (1)$$

The global electrophilicity ω for dipoles and dipolophilic was evaluated using Eq. (2):²⁷

$$\omega = \mu^2/2(\epsilon_{\text{LUMO}} - \epsilon_{\text{HOMO}}) \quad (2)$$

As usual, local indexes are computed in atomic condensed form.²⁸ The well-known Fukui function^{29,30} for electrophilic (f_k^-) and nucleophilic attack (f_k^+) can be written as

$$f_k^- = [q_k(N) - q_k(N-1)] \quad (3)$$

$$(f_k^+) = [q_k(N+1) - q_k(N)] \quad (4)$$

Where $q_k(N)$, $q_k(N-1)$ and $q_k(N+1)$ are the electronic population of the site k in neutral, cationic, and anionic systems, respectively. The local electrophilicity index, ω_k , condensed to atom k is easily obtained by projecting the global quantity onto any atomic centre k in the

molecule by using the electrophilic Fukui function (e.g. the Fukui function for nucleophilic attack, f_k^+)³¹

$$\omega = \omega f_k^+ \quad (5)$$

Domingo et al. has introduced an empirical (relative) nucleophilicity index, N,³² based on the HOMO energies obtained within the Kohn–Sham scheme,²⁶ and defined as:

$$N = \epsilon_{\text{HOMO}}(Nu) - \epsilon_{\text{HOMO}}(TCE) \quad (6)$$

This nucleophilicity scale is referred to tetracyanoethylene (TCE) taken as a reference. Local nucleophilicity index,³³ N_k, was evaluated using the following equation:

$$N_k = N f_k^- \quad (7)$$

Where f_k^- is the Fukui function for an electrophilic attack.^{29,30}

3. Results and Discussion

3. 1. Activation Energy Calculations

The transition states have been localized for both cyclization modes. The corresponding activation energies and structures are given in Table 1 and Figure 1, respectively. Analysis of the geometries at the TS structures given in Figure 1 shows that they correspond to asynchronous bond formation processes. The extent of bond formation along a reaction pathway is provided by the concept of bond order (BO).³⁴ The BO (Wiberg indexes) values of the N–C and C–C forming bonds at TS-

s are shown in brackets in Figure 1. These values are within the range of 0.03 to 0.37. The BO analysis shows that these TSs correspond to asynchronous concerted processes.

In the gas phase, the results show that the **TS3a** is more asynchronous than the **TS4a**, the **TS3b** is more asynchronous than the **TS4b** and the **TS3c** is more asynchronous than the **TS4c**. In general, the asynchronicity shown by the geometrical data is accounted by the BO values. All reactions are exothermic with large ΔE_r (relative energies between products and reactants) energy values. According to Hammond's postulate, the TSs should then be closer to the reactants and can also be interpreted in terms of the position of the transition state along the reaction coordinate, n_T , as defined by Agmon:³⁵

$$n_T = \frac{1}{2 - (\Delta G_r^\# / \Delta G_r)} \quad (8)$$

Where $\Delta G^\#$ and ΔG_r are the relative Gibbs free energy change between the reactants and their corresponding transition states and relative Gibbs free energy change between products and reactants respectively.

The extent of n_T shows the degree of similarity between the transition state and the product. According to the equation 8, the situation of the transition state along the reaction coordinate is determined exclusively by ΔG_r (a thermodynamic quantity) and $\Delta G^\#$ (a kinetic quantity). If $n_T < 0.5$, the transition state is similar to reactants (early TS) and if $n_T > 0.5$, the transition state is similar to products (late TS).³⁵ The values of n_T for these 1,3-DCs are

0.2604 (for **1a + 2 → 3a**), 0.2953 (for **1a + 2 → 4a**), 0.2545 (for **1b + 2 → 3b**), 0.2924 (for **1b + 2 → 4b**), 0.2562 (for **1c + 2 → 3c**), and 0.2942 (for **1c + 2 → 4c**). Therefore, we can conclude that TSs in all these reactions should be closer to the reactants. As it can be seen in Table 1, **TS3a** is located 13.7 kcal below **TS4a**, **TS3b** is located 13.5 kcal below **TS4b** and **TS3c** is located 14.0 kcal below **TS4c**. Thus, regioisomers **3a–c** are kinetically more favored than regioisomers **4a–c**. Furthermore, the presence of the CF₃ group in nitrilimine **1c** slightly increases the barrier.

The comparison of the results presented in Table 1 with above mentioned BO values reveals a relationship between the activation energy of the TS structures and the asynchronicity of the reactions. Less energetic transition states **TS3a–c** are more asynchronous than **TS4a–c**. This findings are in line with the empirical rule that holds for a variety of [4 + 2] cycloaddition reactions that “for asymmetrically substituted dienophiles, the more asynchronous TS has the lower energy”.^{36–38}

The evaluation of the electronic nature of these 1,3-DC reactions showed that the atomic charges in the transition state were shared between the dipoles **1a–c** and **2** (see Figure 1). In the gas phase, the charge transfer (CT) in the transition state, which fluxes from the dipolarophile **2** to the dipoles **1a–c**, ranges from 0.06 to 0.18 e, indicating the polar nature of the 1,3-DC reactions.

IRC calculations were carried out for all studied reactions, and presented only for the reaction between **1a** and **2** at the pathway leading to **3a** (Figure 2). This figure shows saddle point clearly, and demonstrates that the TS

Table 1. Energies of reactants, transition states and cycloadducts **3a–c** and **4a–c**, E (a.u.), relative activation energies, ΔE_a (kcalmol⁻¹), relative Gibbs free energy change between the reactants and their corresponding transition states, $\Delta G^\#$ (kcalmol⁻¹), relative energies between products and reactants, ΔE_r (kcalmol⁻¹), and relative Gibbs free energy change between products and reactants ΔG_r (kcalmol⁻¹).

Reaction	System	E	ΔE_a^a	$\Delta G^\# a$	ΔE_r^a	ΔG_r^a
1a + 2	1a	-532.5441				
	2	-1240.5913				
	TS 3a	-1773.1240	7.19	21.45		
	TS 4a	-1773.1022	20.86	35.26		
	3a	-1773.1949			-44.53	-39.46
1b + 2	4a	-1773.1881			-53.91	-48.87
	1b	-571.8718				
	2	-1240.5913				
	TS 3b	-1812.4513	7.37	20.44		
	TS 4b	-1812.4298	20.83	34.27		
1c + 2	3b	-1812.5222			-44.50	-39.43
	4b	-1812.5153			-53.66	-48.66
	1c	-869.6831				
	2	-1240.5913				
	TS 3c	-2110.2641	6.46	20.53		
	TS 4c	-2110.2418	20.45	35.05		
	3c	-2110.3351			-44.59	-39.06
	4c	-2110.3280			-54.09	-49.02

^a Relative to the reactants.

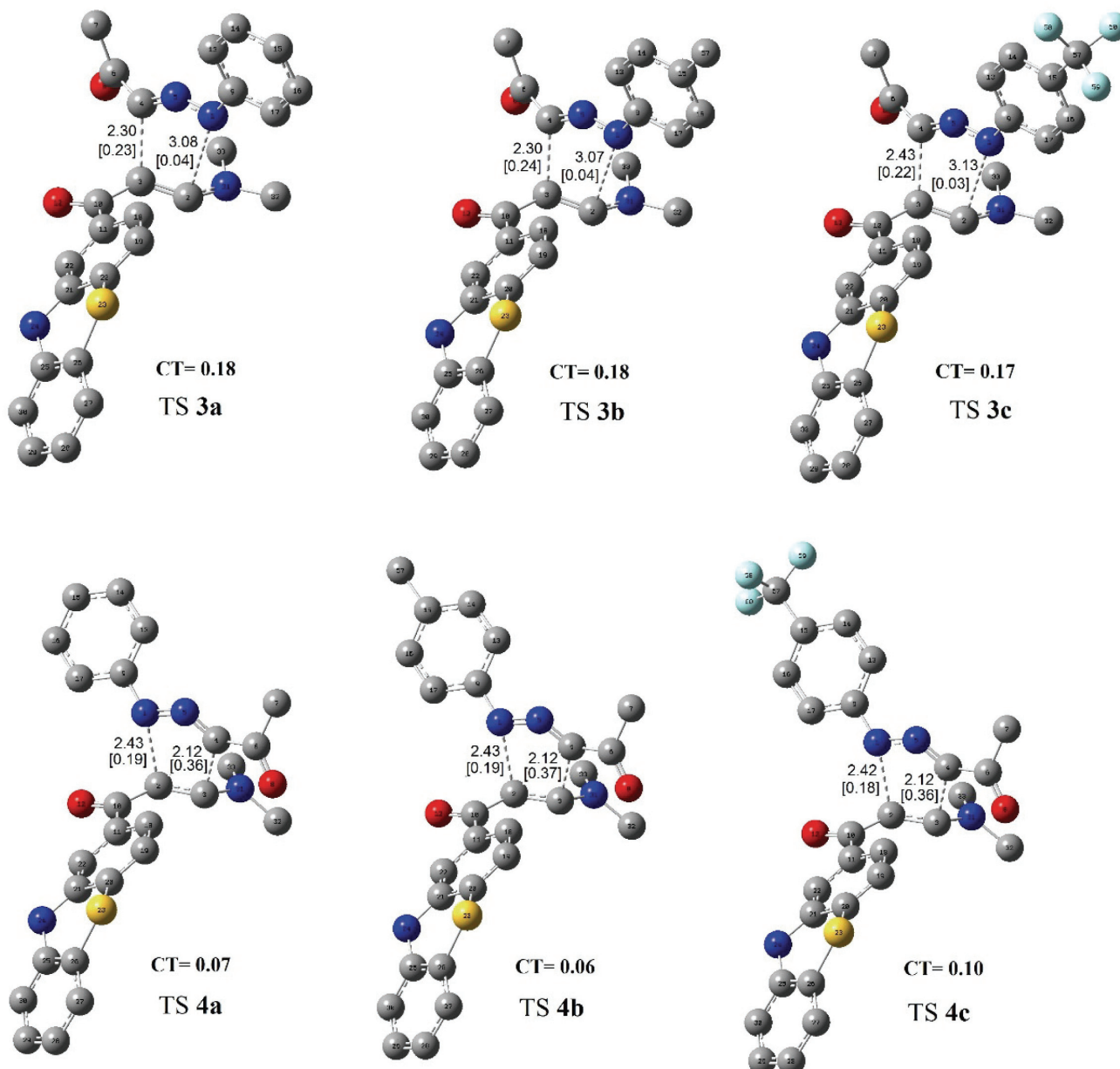


Figure 1. The optimized geometries for transition state structures at the B3LYP/6-311G (d,p) level of theory. Hydrogen atoms have been omitted for clarity. Distances of forming bonds are given in angstroms. The bond orders are given in brackets.

connect to the associated minima of the concerted mechanism.

3. 2. Distortion/interaction Model

Bickelhaupt (activation/strain model),³⁹ and Houk (distortion/interaction model),⁴⁰ independently developed an useful model to understand different issues such as reactivity trends and TS geometries. According to this model, the activation energy (ΔE^\ddagger) is decomposed into two main components: the distortion energy (ΔE_d^\ddagger , also known as the strain energy) and the interaction energy

(ΔE_i^\ddagger , as shown in Eq. (9)):

$$\Delta E^\ddagger = \Delta E_d^\ddagger + \Delta E_i^\ddagger \quad (9)$$

Where ΔE_a^\ddagger and ΔE_i^\ddagger are the energies required to distort the reactants from their initial geometries to their transition state geometries and the binding energy between the deformed reactants in the transition state respectively.⁴¹

In Figure 3 are shown the values computed for ΔE^\ddagger , ΔE_d^\ddagger and ΔE_i^\ddagger and dissected as the sum of the 1,3-dipole distortion energy ($\Delta E_{d-dipole}^\ddagger$) and the dipolarophile distortion

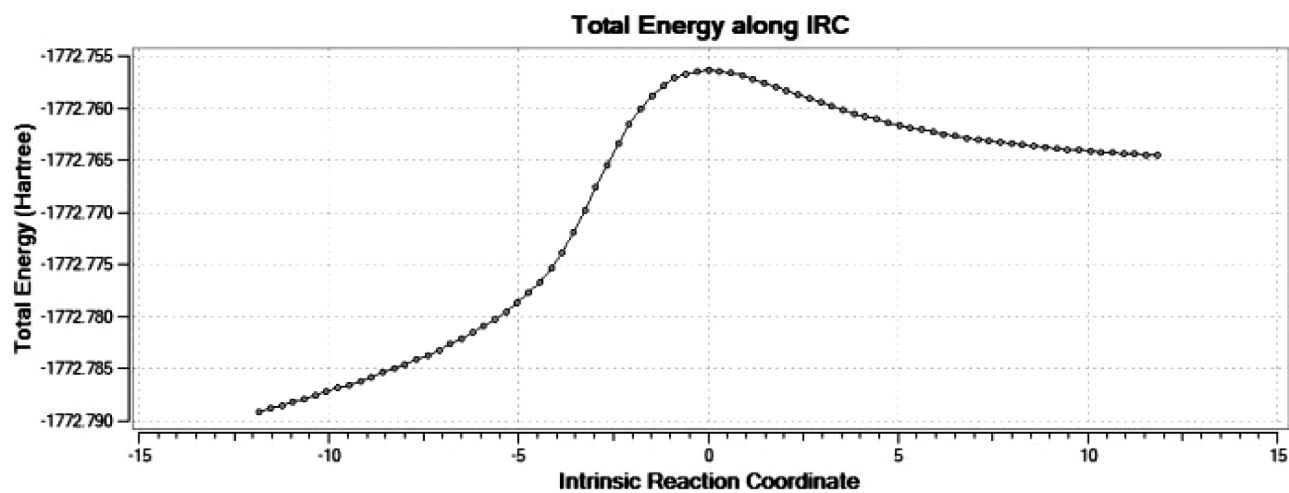


Figure 2. B3LYP/6-311G (d,p) IRC plot for the pathway of 1,3-DC reaction between **1a** and **2** leading to **3a**.

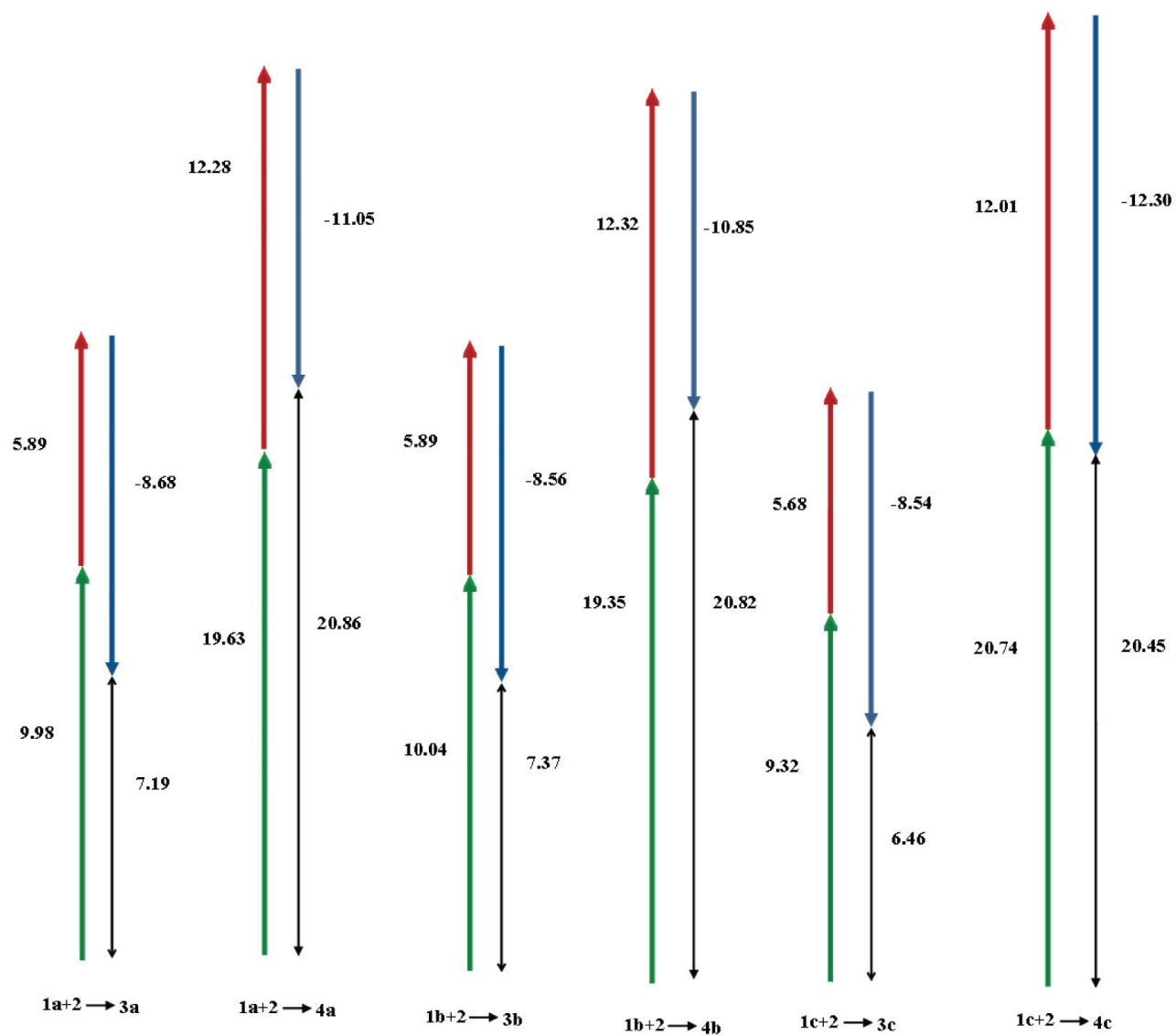


Figure 3. Values of ΔE^\ddagger (black line), $\Delta E^\ddagger_{d\text{-}dipole}$ (green line), $\Delta E^\ddagger_{d\text{-}dipolarophile}$ (red line) and ΔE^\ddagger_i (blue line) for the studied 1,3-DCs.

energy ($\Delta E_{d-dipolarophile}^\ddagger$).

Ess and Houk reported that “the energy to distort the 1, 3-dipole and dipolarophile to the transition state geometry is the major factor controlling the reactivity differences of 1,3-dipoles. Interaction energies between the 1, 3-dipole and the dipolarophile differentiate reactivity for a series of substituted alkenes when the distortion energies are nearly constant.”⁴⁰ As shown in Figure 3, the $\Delta E_{d-dipole}^\ddagger$ is the most pertinent factor, including ~85% of the distortion energy. The $\Delta E_{d-dipole}^\ddagger$ value for **3a–c** formation is smaller than that for **4a–c**. The later transition state means that greater geometrical deformation of reactants requires more distortion energy. Therefore, we can conclude that the distortion energy values favor the formation of the cycloadducts **3a–c** against their regioisomers **4a–c** respectively. Furthermore, Sarotti showed that highly asynchronous TS is predicted to be considerably less distorted than more synchronous one.⁴¹ According to this finding, as shown in Figure 3 and discussed in section 3.1, the TS**3a–c** are more asynchronous than TS**4a–c**. In general, the asynchronicity shown by the geometrical data in section 3.1 agrees with the reactivity trends experimentally observed and predicted by distortion energies.

3. 3. DFT-based Reactivity Indexes

As it can be seen in Table 2, the electronic chemical potential (μ) of dipolarophile **2** (-0.1216) is greater than those of dipoles **1a** (-0.1246), **1b** (-0.1479) and **1c** (-0.1665), thereby suggesting that the net charge-transfer will take place from the dipolarophile **2** to dipoles **1a–c**. This indicates that dipoles **1a–c** will more likely behave as electron acceptor species (i.e. as electrophile). These results are in agreement with CT calculations at the TSs.

The difference in electrophilicity for the dipole/dipolarophile pair, $\Delta\omega$, was found to be a measure of the high- or low-polar character of the cycloaddition.⁴² The small $\Delta\omega$ between **1a** and **2** (0.98 eV), and 0.82 eV for **1b** + **2**, shows a low-polar character for these 1,3-DC reactions, but the presence of CF₃ group (an electron-withdrawing group) on phenyl ring in dipole **1c**, not only increases $\Delta\omega$ (1.35) but also, in comparison to the dipoles **1a** and **1b**, enhances electrophilicity (ω) and reduces nucleophilicity (N).

The Fukui indexes for the atoms N1 and C3 of the dipoles **1a–c** and for the atoms C4 and C5 of the dipolarophile **2** are given in Table 3 (see Figure 4 for atom numbering). Computed Fukui functions are based on the MK electronic population.

Table 3. Fukui indexes for N1 and C3 atoms of the dipoles **1a–c** and for atoms C4 and C5 of the dipolarophile **2**.

Reactants	Atom number	f_k^-	f_k^+
1a	N1	0.0792	
	C3	0.1053	
1b	N1	0.0788	
	C3	0.1045	
1c	N1	0.0660	
	C3	0.0981	
2	C4	0.0252	
	C5	0.0211	

In Figure 4 are reported values of local electrophilicities ω_k for atoms N1 and C3 of the dipoles **1a–c** and local electrophilicities N_k for atoms C4 and C5 of the dipolarophile **2**. According to the Domingo's model,^{31,32} in a polar cycloaddition reaction between unsymmetrical reagents, the more favorable two-centre interaction will take place between the more electrophilic center, characterized by the highest value of the local electrophilicity index ω_k at the electrophile, and the more nucleophilic center characterized by the highest value of the local nucleophilicity index N_k at the nucleophile. These results show that the two-center polar model, based on electrostatic charges, correctly predicts experimental regioselectivity.

4. Conclusion

Mechanism of the 1,3-dipolar cycloaddition reactions of *E*-3-(dimethylamino)-1-(10*H*-phenothiazin-2-yl) prop-2-en-1-ones **1a–c** with nitrilimine **2** has been investigated using activation energy calculations, distortion/interaction model and DFT-based reactivity indexes at the B3LYP/6-311G (d,p) level of theory. The results of this work clearly support the experimentally observed regiochemistry.

Table 2. HOMO and LUMO energies in a.u., electronic chemical potential (μ in a.u.), chemical hardness (η in a.u.), global electrophilicity (ω , in eV) and global nucleophilicity (N, in eV) for reactants **1a–c** and **2**.

Reactants	ϵ_{HOMO}	ϵ_{LUMO}	μ	η	ω	N ^a
1a	-0.2248	-0.0244	-0.1246	0.2004	1.05	3.00
1b	-0.2192	-0.0766	-0.1479	0.1426	2.09	3.16
1c	-0.2387	-0.0944	-0.1665	0.1443	2.61	2.63
2	-0.1888	-0.0545	-0.1216	0.1343	1.49	3.98

^a The HOMO energy of tetracyanoethylene is -0.3351 a.u. at the same level of theory.

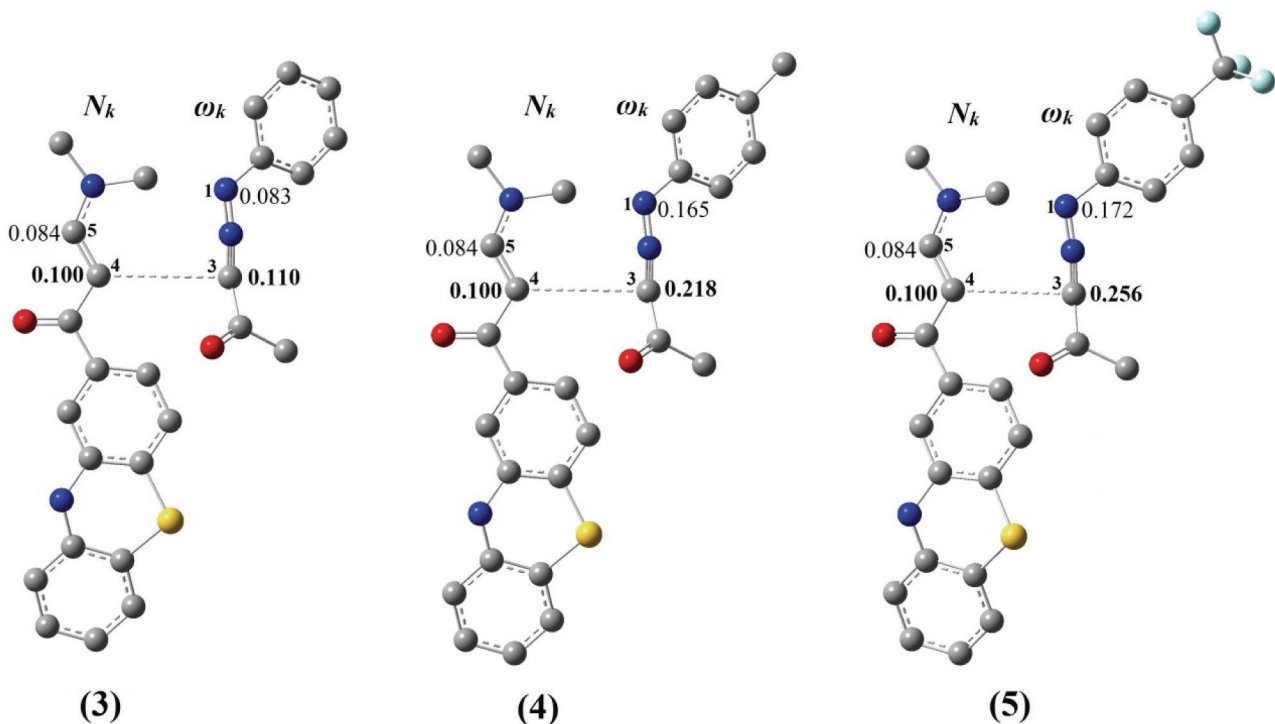


Figure 4. Illustration of the favorable interactions using local nucleophilicities, N_k and local electrophilicities, ω_k .

5. Acknowledgments

The authors are grateful to Islamic Azad University, Bandar Abbas and Mashhad Branches for financial support.

6. References

- K. V. Gothelf, K. A. Jorgensen, *Chem. Rev.* **1998**, *98*, 863–910. <http://dx.doi.org/10.1021/cr970324e>
- A. Padwa, *1,3-Dipolar Cycloaddition Chemistry*; Wiley-Interscience, New York, 1984.
- L. R. Domingo, M. J. Aurell, J. A. Saez, *J. Org. Chem.* **2007**, *72*, 4220–4227. <http://dx.doi.org/10.1021/jo070373j>
- G. O. Jones, K. N. Houk, *J. Org. Chem.* **2008**, *73*, 1333–2342. <http://dx.doi.org/10.1021/jo702295d>
- O. Bortolini, M. D'Agostini, A. DeNino, L. Maiuolo, M. Nardi, G. Sindona, *Tetrahedron* **2008**, *64*, 8078–8081. <http://dx.doi.org/10.1016/j.tet.2008.06.074>
- A. Banerji, P. Sengupta, *J. Indian Inst. Sci.* **2001**, *81*, 313–323.
- G. Molteni, A. Ponti, *Tetrahedron* **2003**, *59*, 5225–5229. [http://dx.doi.org/10.1016/S0040-4020\(03\)00774-9](http://dx.doi.org/10.1016/S0040-4020(03)00774-9)
- G. Molteni, *ARKIVOC* **2007**, *2*, 224–246. <http://dx.doi.org/10.3998/ark.5550190.0008.207>
- A. E. Mekky, T. S. Saleh, A. S. Al-Bogami, *Tetrahedron* **2013**, *69*, 6787–6798. <http://dx.doi.org/10.1016/j.tet.2013.06.028>
- F. Moeinpour, M. Bakavoli, A. Davoodnia, A. Morsali, *J. Theo. Comput. Chem.* **2012**, *11*, 99–109.
- M. Bakavoli, F. Moeinpour, A. Davoodnia, A. Morsali, *J. Mol. Struct.* **2010**, *969*, 139–144. <http://dx.doi.org/10.1016/j.molstruc.2010.01.059>
- F. Moeinpour, *Chin. J. Chem. Phys.* **2010**, *23*, 165–168. <http://dx.doi.org/10.1088/1674-0068/23/02/165-168>
- N. Dorostkar-Ahmadi, M. Bakavoli, F. Moeinpour, A. Davoodnia, *Spectrochim. Acta A* **2011**, *79*, 1375–1380. <http://dx.doi.org/10.1016/j.saa.2011.04.071>
- F. Moeinpour, *Chin. J. Chem.* **2011**, *29*, 1429–1433. <http://dx.doi.org/10.1002/cjoc.201180262>
- M. Bakavoli, F. Moeinpour, A. Davoodnia, A. Morsali, *Chin. J. Chem.* **2011**, *29*, 1167–1172. <http://dx.doi.org/10.1002/cjoc.201190218>
- F. Moeinpour, M. Bakavoli, A. Davoodnia, A. Morsali, *J. Chil. Chem. Soc.* **2011**, *56*, 870–874. <http://dx.doi.org/10.4067/S0717-97072011000400010>
- M. Bakavoli, F. Moeinpour, A. Sardashti-Birjandi, A. Davoodnia, *J. Heterocyclic Chem.* **2013**, *50*, 188–193.
- A. Izadyar, M. Bakavoli, F. Moeinpour, A. Davoodnia, *Res. Chem. Intermed.* <http://dx.doi.org/10.1007/s11164-013-1196-y>
- J. R. Cheeseman, J. A. Montgomery, T. Vreven, K. N. Kudin; J. C. Burant, J. M. Millam, S. S. Iyengar, J. Tomasi, V. Barone, B. Mennucci, M. Cossi, G. Scalmani, N. Rega, G.A. Petersson, H. Nakatsuji, M. Hada, M. Ehara, K. Toyota; R. Fukuda, J. Hasegawa, M. Ishida, T. Nakajima, Y. Honda, O. Kitao, H. Nakai, M. Klene, X. Li, J. E. Knox, H. P. Hratchian,

- J.B. Cross, V. Bakken, C. Adamo, J. Jaramillo, R. Gomperts, R. E. Stratmann, O. Yazyev, A. J. Austin, R. Cammi, C. Pomelli, J. W. Ochterski, P. Y. Ayala, K. Morokuma, G.A. Voth, P. Salvador, J. J. Dannenberg, V. G. Zakrzewski, S. Dapprich, A. D. Daniels, M. C. Strain, O. Farkas, D. K. Malick, A. D. Rabuck, K. Raghavachari, J. B. Foresman, J. V. Ortiz, Q. Cui, A.G. Baboul, S. Clifford, J. Cioslowski, B. B. Stefanov, G. Liu, A. Liashenko, P. Piskorz, I. Komaromi, R. L. Martin, D.J. Fox, T. Keith, M. A. Al-Laham, C. Y. Peng, A. Nanayakkara, M. Challacombe, P. M .W. Gill, B. Johnson, W. Chen, M. W. Wong, C. Gonzalez, J. A. Pople, Gaussian03, Revision B.03, Gaussian, Inc. Pittsburgh, PA, 2003.
20. H. B. Schlegel, *J. Comput. Chem.* **1982**, *3*, 214–218.
<http://dx.doi.org/10.1002/jcc.540030212>
21. M. H. Gordon, J. A. Pople, *J. Chem. Phys.* **1988**, *89*, 5777–5786. <http://dx.doi.org/10.1063/1.455553>
22. C. González, H. B. Schlegel, *J. Phys. Chem.* **1990**, *94*, 5523–5527. <http://dx.doi.org/10.1021/j100377a021>
23. C. González, H. B. Schlegel, *J. Chem. Phys.* **1991**, *95*, 5853–5860. <http://dx.doi.org/10.1063/1.461606>
24. U. C. Singh, P. A. Kollman, *J. Comput. Chem.* **1984**, *5*, 129–145. <http://dx.doi.org/10.1002/jcc.540050204>
25. B. H. Besler, K. M. Merz, P. A. Kollman, *J. Comput. Chem.* **1990**, *11*, 431–439.
<http://dx.doi.org/10.1002/jcc.540110404>
26. R. G. Parr, R. G. Pearson, *J. Am. Chem. Soc.* **1983**, *105*, 7512–7516. <http://dx.doi.org/10.1021/ja00364a005>
27. R. G. Parr, L. Von Szentpaly, S. Liu, *J. Am. Chem. Soc.* **1999**, *121*, 1922–1924. <http://dx.doi.org/10.1021/ja983494x>
28. W. Yang, W. J. Mortier, *J. Am. Chem. Soc.* **1986**, *108*, 5708–5711. <http://dx.doi.org/10.1021/ja00279a008>
29. K. Fukui, *Science* **1982**, *218*, 747–750.
<http://dx.doi.org/10.1126/science.218.4574.747>
30. R. G. Parr, W. Yang, *J. Am. Chem. Soc.* **1984**, *106*, 4049–4050.
<http://dx.doi.org/10.1021/ja00326a036>
31. L. R. Domingo, M. J. Aurell, P. Pérez, *J. Phys. Chem. A* **2002**, *106*, 6871–6875. <http://dx.doi.org/10.1021/jp020715j>
32. L. R. Domingo, P. Pérez, *J. Org. Chem.* **2008**, *73*, 4615–2446.
<http://dx.doi.org/10.1021/jo800572a>
33. E. Chamorro , M. Duque-Noreña, P. Pérez, , *J. Mol. Struct.: (THEOCHEM)* **2009**, *896*, 73–79.
<http://dx.doi.org/10.1016/j.theochem.2008.11.009>
34. K. B. Wiberg, *Tetrahedron* **1968**, *24*, 1083–1096.
[http://dx.doi.org/10.1016/0040-4020\(68\)88057-3](http://dx.doi.org/10.1016/0040-4020(68)88057-3)
35. N. Agmon, R. D. Levine, *Chem. Phys. Lett.* **1977**, *52*, 197–201. [http://dx.doi.org/10.1016/0009-2614\(77\)80523-X](http://dx.doi.org/10.1016/0009-2614(77)80523-X)
36. J. I. García, V. Martínez-Merino, J. A. Mayoral, L. Salvatella, *J. Am. Chem. Soc.* **1998**, *120*, 2415–2420.
<http://dx.doi.org/10.1021/ja9722279>
37. L. R. Domingo, M. Arno', J. Andre's, *J. Org. Chem.* **1999**, *64*, 5867–5875. <http://dx.doi.org/10.1021/jo990331y>
38. L. R. Domingo, *Eur. J. Org. Chem.* **2000**, *12*, 2265–2272.
[http://dx.doi.org/10.1002/1099-0690\(200006\)2000:12<2265::AID-EJOC2265>3.0.CO;2-C](http://dx.doi.org/10.1002/1099-0690(200006)2000:12<2265::AID-EJOC2265>3.0.CO;2-C)
39. I. Fernández, M. Solà, F. M. Bickelhaupt, *Chem. Eur. J.* **2013**, *19*, 7416–7422.
<http://dx.doi.org/10.1002/chem.201300648>
40. D. H. Ess, K. N. Houk *J. Am. Chem. Soc.* **2008**, *130*, 10187–10198. <http://dx.doi.org/10.1021/ja800009z>
41. A. M. Sarotti, *Org. Biomol. Chem.* DOI: 10.1039/C3O B41628C. <http://dx.doi.org/10.1039/C3OB41628C>
42. H. Chemouri, S. M. Mekelleche, *Int. J. Quantum Chem.* **2012**, *112*, 2294–2300. <http://dx.doi.org/10.1002/qua.23232>

Povzetek

V prispevku je opisana raziskava regiokemijskega poteka 1,3-cikoadicijskih reakcij *E*-3-(dimetilamino)-1-(10*H*-fenotiazin-2-il) prop-2-en-1-ona z nekaterimi nitrilimini, ki je bila narejena z uporabo reaktivnostnih indeksov, izračunom aktivacijske energije in modelom popočenja/interakcije na osnovi teorije gostotnega funkcionala (DFT) in uporabe B3LYP/6-311G(d,p) funkcij. Analiza geometrije prehodnih stanj in reda vezi struktur, ki so povezane z različnimi reakcijskimi potmi, kaže na to, da te 1,3-dipolarne cikloadicijke reakcije potekajo preko asinhronega koncertiranega mehanizma.